Saturation of harmonic generation in one- and three-dimensional atoms

S. C. Rae, X. Chen, and K. Burnett
Clarendon Laboratory, Department of Physics, University of Oxford, Oxford OX1 3PU, United Kingdom
(Received 8 July 1993; revised manuscript received 22 March 1994)

A commonly used numerical technique for calculating the harmonic spectrum emitted by an atom exposed to an intense laser pulse is the direct integration of the Schrödinger equation. We compare the spectra calculated using two different models. The first is in one dimension with an approximate hydrogenic soft-core potential and the second is in three dimensions with a Coulomb potential. We use realistic laser pulse conditions (100 fs, 800 nm) and intensities at which there is significant ionization, leading to a saturation of the harmonic-generation process. Although the ionization rates in the two models differ, the harmonic spectra and the positions of the cutoff are remarkably similar. Only a relatively small number of angular momentum states is needed in the three-dimensional calculation to give a reliable estimate of the cutoff, even for intensities at which there is strong ionization.

PACS number(s): 42.50.Hz, 32.80.Rm, 42.65.Ky

An atom exposed to a high-intensity laser pulse radiates a series of odd harmonics of the fundamental frequency. This phenomenon of harmonic generation has been observed over wide ranges of laser intensity and wavelength and for many different atomic species. Much of the recent interest in harmonics has centered on the production of the shortest possible wavelengths, with several groups reporting the generation of radiation near or below 10 nm [1–4].

Theoretically, it is a major challenge to describe atomic dynamics in an intense short-pulse laser field. A number of distinct approaches to this problem have been developed, one of the most useful being direct integration of the time-dependent Schrödinger equation (TDSE). However, the atomic response is only a part of the problem, and propagation effects are equally important in determining the actual spectrum recorded in an experiment. Due to the extreme computational demands, solutions of the combined atomic response and propagation equations have so far only been obtained in a slowly-varying-envelope (SVE) approximation [5]. However, for recent experiments performed with laser pulse durations much less than 1 ps, the SVE approximation is no longer appropriate and the propagation equations would have to be solved in their full time-dependent form. In order to make numerical solution of such equations feasible, it is, therefore, most important to find the simplest atomic models that are capable of describing the atomic behaviour of interest. This paper compares the results from a number of such simple models.

The regime where the maximum number of harmonics have been found in experiments corresponds to the onset of strong ionization. The observation of plasma-induced blueshifting of harmonics in this regime [1] clearly demonstrates that ionization and high-order harmonic generation are closely linked. In this paper we compare two different methods for calculating atomic response in the strongly ionizing regime, based on the numerical integration of the TDSE in one or three dimensions. We show that relatively simple models can be quite successful in predicting key features, for example, the ionization rate and the cutoff in the high-harmonic spectrum.

Several problems conspire to make numerical solutions of the TDSE at high intensities difficult to obtain. The first of these is simply the time scale on which the wave function evolves. For a short pulse, ionization may occur rapidly over a relatively small number of laser cycles and the numerical integration consequently requires hundreds or maybe thousands of steps per cycle [6,7]. The second major problem arises because of the finite size of the numerical grid used in the calculation. Parts of the wave function which move far from the core tend to be reflected from the edge of the numerical grid and reinteract with the core, generating spurious harmonics. This unwanted reflection can be eliminated mathematically by using an absorber or mask function which smoothly reduces the wave function to zero at the edge of the grid. In a one-dimensional (1D) calculation, a frame of reference can be chosen, the Kramers-Henneberger (KH) frame, in which the wave function reaching the edge of the grid is freely diffusing. This slowly moving part of the wave function can then be efficiently absorbed [7]. Outside a 1D approximation, however, this is not generally possible. In this case the wave function which reaches the edge of the grid is still oscillating in the laser field and can be moving with a high velocity, making a good absorber difficult to implement.

A more fundamental problem is connected with very short duration pulses. Previous calculations have often used a half-trapezoidal pulse shape, with a linear or sine-squared turn on over typically 5 cycles, followed by a constant intensity for 10–20 cycles [6]. Using this method an ionization rate and set of harmonic efficiencies can be defined at a particular (steady state) intensity, and these can subsequently be used, for example, in a SVE propagation code. For the latest generation of short-pulse Ti:sapphire lasers, with pulse lengths approaching 100 fs, such an approach is no longer appropriate. The time history of the pulse is important, and it is not valid to define a response at a particular intensity, only a response to a particular total pulse. This is specifically the regime

we are considering here, and any harmonic spectrum we discuss will always be the spectrum from an entire pulse, as would be measured in a hypothetical single-atom experiment.

We will now briefly outline the two models, before presenting some comparative results and discussing the computational and other problems. A 1D model atom has been extensively investigated in recent years, first by Eberly, Su and Javanainen [8] and subsequently by Reed and Burnett [9], Sanpera and Roso-Franco [10], and others. The TDSE for this case can be written, using atomic units, as

$$i\frac{\partial}{\partial t}\psi(x,t) = -\frac{1}{2}\frac{\partial^2}{\partial x^2}\psi(x,t) + V(x+\alpha(t))\,\psi(x,t)\ . \quad (1)$$

This is expressed in the KH frame, in which the oscillatory motion of a free electron in the field is transferred to the potential. The parameter $\alpha(t)$ represents the instantaneous displacement of the frame. The soft-core potential is of the form

$$V(x) = \frac{-1}{\sqrt{2+x^2}}\ . \quad (2)$$

This potential supports a ground state with a binding energy of 0.5 a.u., so it can be used as an approximation to atomic hydrogen. Various scaled potentials can be developed to represent other species [8], but for this paper we have opted to use a simple case. The aim is not to generate spectra which can be quantitatively compared with experiment (hydrogen has not been used in harmonic generation experiments thus far), but rather to compare the predictions of various atomic models under identical conditions.

The 3D model starts with the full TDSE, including the coupling to the field in length gauge,

$$i\frac{\partial}{\partial t}\psi(\vec{r},t) = \left(-\frac{1}{2}\nabla^2 - \frac{1}{r} + \vec{r}\cdot\vec{E}(t)\sin\omega t\right)\psi(\vec{r},t)\ . \quad (3)$$

Here $E(t)$ is the electric field envelope and the potential is Coulombic, appropriate to atomic hydrogen. For light linearly polarized along the z axis, the wave function can be expanded in spherical harmonics

$$\psi(\vec{r},t) = \sum_{l=0}^{\infty}\frac{1}{r}\chi_l(r,t)\,Y_l^0(\theta)\ , \quad (4)$$

leading to a set of coupled equations for the radial functions

$$i\frac{\partial}{\partial t}\chi_l(r,t) = \left[-\frac{1}{2}\frac{\partial^2}{\partial r^2} - \frac{1}{r} + \frac{l(l+1)}{2r^2}\right]\chi_l(r,t) + rE(t)\sin\omega t\,\left[c_l^+\chi_{l+1}(r,t) + c_l^-\chi_{l-1}(r,t)\right]\ , \quad (5)$$

where the $c_l^{\pm}$ are coupling constants related to Clebsch-Gordan coefficients [11].

Each angular momentum channel l is coupled by the field to channels $l\pm1$ (except $l=0$, which is only coupled to $l=1$). This set of coupled equations can be solved numerically using an efficient split-operator technique, in which the evolution in r and the interchannel coupling in l is performed alternately each half time step. The number of channels is adjustable and thus the model is more properly described as two dimensional in r and l. Such a simple coupling scheme is only obtained if the interaction with the field in Eq. (4) is in length gauge. Although moving to the KH frame would be advantageous for the absorbers, this would be far outweighed by the increased complexity of the interchannel coupling. Length gauge has the advantage that the interaction with the field goes to zero at $r=0$ (where the potential has a singularity), but suffers from problems at large r because the interchannel coupling terms grow without bound.

In both models, the ground state can be found by solving the time-independent Schrödinger equation. This initial state is then evolved numerically under the influence of the laser field and the harmonic spectrum is obtained from a Fourier transform of the dipole acceleration [12], which is calculated using Ehrenfest's theorem as

$$a(t) = \left\langle \psi(t)\left|\frac{-\partial V}{\partial \vec{r}} + E(t)\sin\omega t\right|\psi(t)\right\rangle\ . \quad (6)$$

Because of the absorbing boundaries, the norm of the wave function on the grid decreases with time and we use this as an approximate measure of ionization.

In order to compare the harmonic spectra predicted by the two models, we have performed a series of calculations using a common set of parameters. We assumed a frequency of 0.056 55 a.u. (corresponding to 800 nm, appropriate to Ti:sapphire), a total pulse length of 96 cycles, and a sine-squared pulse envelope (full width at half maximum $\simeq$ 100 fs). The total number of time steps was 65 536 and the space grid consisted of 1200 (3D) or 2400 (1D) points, with a grid spacing of 0.25 a.u. The grid was larger in the 1D case because we need to consider both positive and negative x values; symmetry in 3D halves the number of points required. After each time step, the wave function was multiplied by a $\cos^{1/8}$ mask function, which extended over 200 points at the edge of the grid. The harmonic spectrum was obtained from the dipole acceleration recorded over the entire pulse.

Figure 1 compares the potentials used in the calcu-

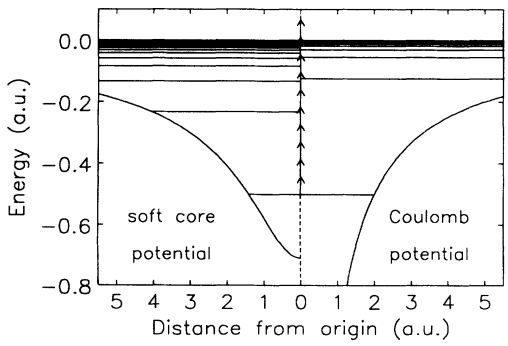

FIG. 1. A comparison of the 1D and 3D potentials, showing the positions of the bound states in each case. Arrows indicate photon energies. Note that the actual grid used for calculations is considerably larger than that shown here.

lations. The binding energy is the same in both cases, although the positions of the excited states differ. At least nine photons are required for ionization. For the chosen grid, there are 29 bound states in the 1D case and 15 bound n states in the 3D case (the total number of states depends on the number of channels included).

Some examples of harmonic spectra are shown in Fig. 2, where we compare the 1D results with those from a 12-channel 3D calculation, at a peak intensity of 10^{14} W/cm^2. These full-pulse spectra typically have much more structure than those obtained with a ramped, constant-intensity pulse and the harmonic peaks have a noticeable width because they are only generated over a limited number of cycles. There are many differences between the 1D and 3D spectra, but qualitatively, especially regarding the position of the high harmonic cutoff, there is close agreement. There is considerably more numerical noise in the 3D case, which is due to less efficient absorbers, as mentioned above. The use of the dipole acceleration (rather than the dipole moment) to obtain the spectrum helps to reduce the effect of reflections because, as Eq. (6) shows, the dipole acceleration is determined only by the component of the wave function near the core (where $\partial V/\partial r$ is large) rather than across the entire grid. The final degree of ionization is markedly different for the two cases shown in the figure: 94% in the 1D model, but only 22% in the 3D model.

In order to have a clear feature with which to compare various spectra, we will use the cutoff harmonic, which we define, somewhat arbitrarily, as the highest order harmonic q which has an intensity greater than 10^{-9} in 1D and 10^{-11} in 3D of the fundamental. Thus, in Fig. 2, the cutoff in both the 1D and 3D cases is at $q = 31$. By plotting the cutoff harmonic as a function of intensity for various cases, we can determine where the 1D model gives acceptable results and see the effect of changing the number of channels in the 3D model. Figure 3 summarizes the results for the 1D model and the 3D model with 4, 12, and 24 channels. In the same figure we also plot the final degree of ionization as a function of intensity.

Examining the ionization results first, it is clear that simply making the ionization potential the same in the two cases is insufficient to obtain identical ionization rates; this is due partly to the changing position of the excited energy levels, but also to fundamentally different behavior in 3D compared to 1D. It is worth stressing, however, that despite the large difference in final ionization, the harmonic spectra appear very similar. The position of the cutoff depends primarily on the intensity and not on the rate of ionization. Increasing the number of channels in the 3D calculation increases the saturation intensity slightly, but does not have a large effect. The difference between 12 and 24 channels is too small to show up on the figure.

The 1D atom generally shows a slightly higher cutoff, except at very high intensities, where the decrease is due to depletion of the neutral. Above about 3×10^{14} W/cm^2, where ionization occurs rapidly in the leading edge of the pulse, the 1D results are poorly converged for this choice of time step and grid spacing, and points beyond this intensity have been omitted. The number of channels required in the 3D case depends on the intensity. Below 10^{14} W/cm^2, 4 channels are sufficient to converge the cutoff harmonic, and only above 3×10^{14} W/cm^2 are 24 channels necessary. Until intensities are reached when ionization occurs completely before the peak of the pulse,

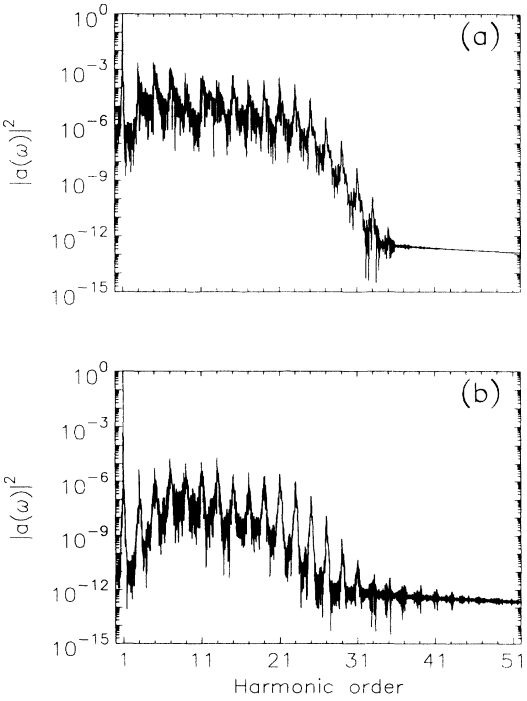

FIG. 2. Example harmonic spectra for (a) a model 1D and (b) a 12-channel 3D hydrogen atom, with a nominal 100 fs, 800 nm laser pulse at a peak intensity of 10^{14} W/cm^2.

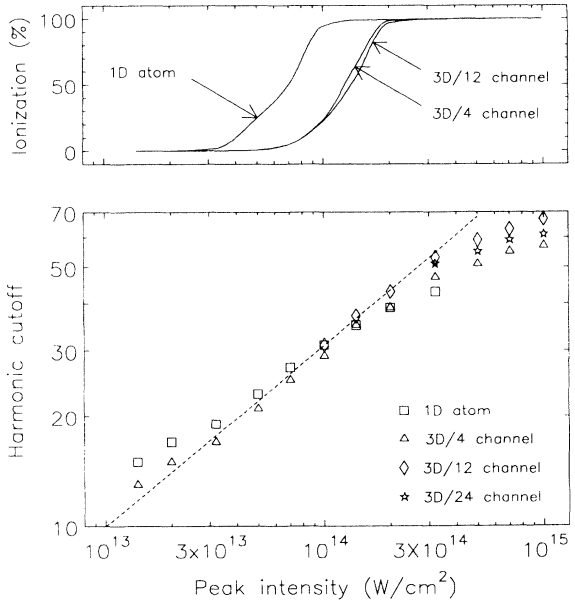

FIG. 3. Dependence of the harmonic cutoff q and the final degree of ionization as functions of peak pulse intensity for the 1D model and the 3D model with 4, 12, and 24 channels. The dotted line indicates the relationship $q = \mathcal{E}_i + 3\mathcal{E}_q$.

the harmonic cutoff in all the various models agrees quite closely with the prediction of simple classical models [13] that $q \simeq \mathcal{E}_i + 3\mathcal{E}_q$, where $\mathcal{E}_i$ is the ionization potential and $\mathcal{E}_q$ is the quiver or ponderomotive energy.

We should point out that although the position of the cutoff, as we have defined it here, is fairly insensitive to the number of channels, the same is not necessarily true of the intensity of individual harmonic peaks. Considerably more than 24 channels would be needed to completely converge all of the harmonic intensities. Our point here is that a crucial feature, the cutoff, can be accurately predicted using a minimum of channels. Indeed, if ionization rate and cutoff position are the primary quantities of interest, a four-channel 3D calculation gives reliable estimates without needing excessive amounts of computer time. It is superior to the 1D model in the prediction of ionization rates, but is only twice as demanding computationally (four channels instead of one, but a radial grid only half the size). Such a model would be well suited for use in a larger non-SVE propagation calculation [14], which would then include the effect of the ionizing medium on the overall harmonic generation efficiency.

This work is part of a program supported by the Science and Engineering Research Council.

[1] J. J. Macklin, J. D. Kmetec, and C. L. Gordon III, Phys. Rev. Lett. **70**, 766 (1993).
[2] A. L'Huillier and P. Balcou, Phys. Rev. Lett. **70**, 774 (1993).
[3] J. K. Crane, M. D. Perry, S. Herman, and R. W. Falcone, Opt. Lett. **17**, 1256 (1992).
[4] N. Sarukura, K. Hata, T. Adachi, R. Nodomi, M. Watanabe, and S. Watanabe, Phys. Rev. A **43**, 1669 (1991).
[5] A. L'Huillier, K. J. Schafer, and K. C. Kulander, J. Phys. B **24**, 3315 (1991); A. L'Huillier, P. Balcou, S. Candel, K. J. Schafer, and K. C. Kulander, Phys. Rev. A **46**, 2778 (1992); P. Balcou, C. Cornaggia, A. S. L. Gomes, L. A. Lompré, and A. L'Huillier, J. Phys. B **25**, 4467 (1992).
[6] J. L. Krause, K. J. Schafer, and K. C. Kulander, Phys. Rev. A **45**, 4998 (1992); Phys. Rev. Lett. **68**, 3535 (1992).
[7] S. C. Rae and K. Burnett, Phys. Rev. A **48**, 2490 (1993).
[8] J. H. Eberly, Q. Su, and J. Javanainen, Phys. Rev. Lett. **62**, 881 (1989); J. Opt. Soc. Am. B **6**, 1289 (1989); J. H. Eberly, Q. Su, J. Javanainen, K. C. Kulander, B. W. Shore, and L. Roso-Franco, J. Mod. Opt. **36**, 829 (1989).
[9] V. C. Reed and K. Burnett, Phys. Rev. A **42**, 3152 (1990); **43**, 6217 (1991); **46**, 424 (1992).
[10] A. Sanpera and L. Roso-Franco, Phys. Rev. A **41**, 6515 (1990); J. Opt. Soc. Am. B **8**, 1568 (1991); A. Sanpera, Q. Su, and L. Roso-Franco, Phys. Rev. A **47**, 2312 (1993).
[11] P. L. DeVries, J. Opt. Soc. Am. B **7**, 517 (1990); K. J. LaGattuta, *ibid.* **7**, 639 (1990); L. Roso-Franco, A. Sanpera, M. Ll. Pons, and L. Plaja, Phys. Rev. A **44**, 4652 (1991).
[12] K. Burnett, V. C. Reed, J. Cooper, and P. L. Knight, Phys. Rev. A **45**, 3347 (1992).
[13] K. C. Kulander, K. J. Schafer, and J. L. Krause, in *Super-Intense Laser-Atom Physics*, Vol. 316 of *NATO Advanced Study Institute, Series B: Physics*, edited by B. Piraux, A. L'Huillier, and K. Rzążewski (Plenum, New York, 1993); P. B. Corkum, Phys. Rev. Lett. **71**, 1994 (1993).
[14] S. C. Rae and K. Burnett, J. Phys. B **26**, 1509 (1993).